



# Cosmic ray effects in the iron meteorite Gebel Kamil and its asymmetric ablation

Carla Taricco<sup>1,2</sup>  · Paolo Colombetti<sup>1</sup> · Neeharika Sinha<sup>3</sup> · Narendra Bhandari<sup>4</sup> · Mario Di Martino<sup>2</sup> · Sara Rubinetti<sup>1,2</sup> · Dario Barghini<sup>1,2</sup> · Salvatore Mancuso<sup>2</sup>

Received: 30 November 2018 / Accepted: 17 April 2019  
© Springer Nature B.V. 2019

**Abstract** We have measured gamma rays emanating from radionuclides produced by cosmic ray interactions in two fragments of Gebel Kamil iron meteorite. Based on the cosmogenic <sup>26</sup>Al activity, it is deduced that one fragment, taken from the narrow edge of the mace-shaped main mass, was exposed close to the surface and the other fragment was located about 73 cm deep inside the meteoroid. No signal due to <sup>44</sup>Ti was detected indicating that it has totally decayed on the Earth after fall of the meteorite and the terrestrial age of the meteorite must be longer than a few centuries. The ablation is shown to be asymmetric around the centre of the meteoroid and the pre-atmospheric mass of the meteoroid has been estimated to be between 30 and 60 tons, consistent with other estimates.

**Keywords** Meteorites · Cosmogenic radionuclides · Methods: gamma-ray spectrometry

## 1 Introduction

An impact crater (about 45 meters in diameter and 16 meters deep overlain by 6 meters of crater-fill material) was identified in southern Egypt in photographs taken by Quick Bird

EO satellite in 2008. Subsequently an Italian-Egyptian expedition team recovered from the site several thousand fragments of an iron meteorite, weighing over 1600 kg. The impact crater, meteorite recovery and features of some of the fragments have been described by Folco et al. (2010, 2011), Di Martino et al. (2014).

Several studies related to the chemical composition, classification, cosmic ray exposure age, terrestrial age etc. of the Gebel Kamil meteorite have been carried out over the past few years. The relevant findings are summarized in Table 1. In context of the present studies related to radionuclides, three parameters are important. The cosmic ray exposure age in interplanetary space and the terrestrial age after its fall on the Earth determine the radionuclides which will attain secular equilibrium in space and those which will survive after the fall over its terrestrial residence time. Besides, the shielding depths of the samples determine the rates of production of the radioisotopes. Ott et al. (2014) determined the cosmic ray exposure age of the meteoroid in interplanetary space, based on their work on cosmogenic rare gases and the <sup>36</sup>Cl/<sup>36</sup>Ar method, to be 366 ± 18 Ma. The terrestrial age has been determined to be 3000 ± 600 years by Sighinolfi et al. (2015) using the thermoluminescence dating method.

## 2 Experimental methods

### 2.1 Sample description

Two fragments of Gebel Kamil meteorite, GK1 (672 g) and GK2 (450 g), were available to us for non-destructive measurement of their gamma activity. The first fragment (GK1, Fig. 1) was found near the crater; the second one (GK2) was broken from the 83 kg main body (*the individual*) shown in Fig. 2.

✉ C. Taricco  
carla.taricco@unito.it

<sup>1</sup> Dipartimento di Fisica Generale, Università di Torino, Via Pietro Giuria 1, 10125, Torino, Italy

<sup>2</sup> Istituto Nazionale di Astrofisica - Osservatorio Astrofisico di Torino, Strada Osservatorio 20, 10025, Pino Torinese (TO), Italy

<sup>3</sup> Wentworth Institute of Technology, 550 Huntington Ave, Boston, MA 02115, USA

<sup>4</sup> Science and Spirituality Research Institute, Vijay Crossing, Navrangpura, Ahmedabad, India

**Table 1** Some relevant data about the Gebel Kamil iron meteorite

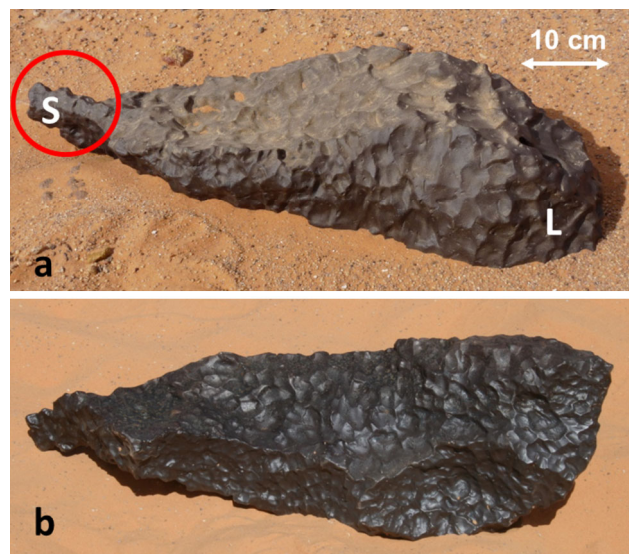
Classification	Ni rich Ataxite	D’Orazio et al. (2011)
Recovered mass	>3000 kg	Folco et al. (2010, 2015)
Pre-atmospheric mass	30 to 60 tons	Ott et al. (2014), This work
Pre-atmospheric radius	1.2 m	Ott et al. (2014), This work
Ablation	>95%	This work
Cosmic ray exposure age	$366 \pm 18$ Ma	Ott et al. (2014)
Terrestrial age	$3000 \pm 600$ a	Sighinolfi et al. (2015)

**Fig. 1** Gebel Kamil meteorite sample GK1 (672 g) studied at the Laboratory of Monte dei Cappuccini (Torino, Italy, OATo – INAF)

We present here the gamma-activity measurements of these two fragments with the aim of obtaining from cosmogenic radionuclides additional information about the pre-atmospheric size of the meteoroid and the shielding depths of the fragments.

## 2.2 Gamma ray spectrometer system and counting details

The samples were counted for gamma activities in a two dimensional (energy-energy mode), highly sensitive, low background, coincidence/anti coincidence double detector gamma ray spectrometer. This highly selective HPGe-NaI(Tl) spectrometer for non-destructive measurement of meteorite samples up to 1 kg is operative in the underground Laboratory of Monte dei Cappuccini (OATo – INAF) in Torino, Italy. A detailed description of the system is given in Taricco et al. (2007) and Colombetti et al. (2008, 2013). Briefly, the system consists of a large volume, high-efficiency hyperpure Ge detector (3 kg), with an umbrella of a well type NaI(Tl) scintillator (90 kg) and a thick sequential Pb-Cd-Cu passive shield, for absorption of ambient radiation by decreasing their energy. The energies of gamma rays detected in the Ge detector are recorded in coincidence together with the energies in the NaI scintillator. Thus highly

**Fig. 2** Two sides (a, b) of the 83 kg main body (called *individual*) of Gebel Kamil meteorite. Sample GK2 (450 g, red circle) was taken from the narrowest end of this body (S), found to be the least ablated part, based on this work

specific energy regions can be selected for measurement. The system is situated in the underground laboratory having 70 m.w.e. (Meters Water Equivalent) of soil overburden to minimize the cosmic ray background. The detector chamber is maintained under continuous flow of nitrogen to flush out the ambient radon, a source of radiation, generated by decay of natural U and Th present in the surrounding rocks and soil. As can be seen from Fig. 3, the background in coincidence mode (blue curve) decreases by more than a factor of 20 compared to the normal mode (black curve), with relatively much smaller reduction in counting efficiency for radionuclides which give coincident gamma rays. The system is very stable for long periods of time (months) as can be determined by the resolution for various background peaks. A very low background is achieved in this way and the typical coincidence background in energy peaks of interest is about a count per day. This highly selective spectrometer allows us to measure low activity levels of cosmogenic radioisotopes that we used for monitoring solar activity over the past centuries (Taricco et al. 2006, 2008, 2016; Usoskin et al. 2006; Asvestari et al. 2017; Mancuso et al. 2018).

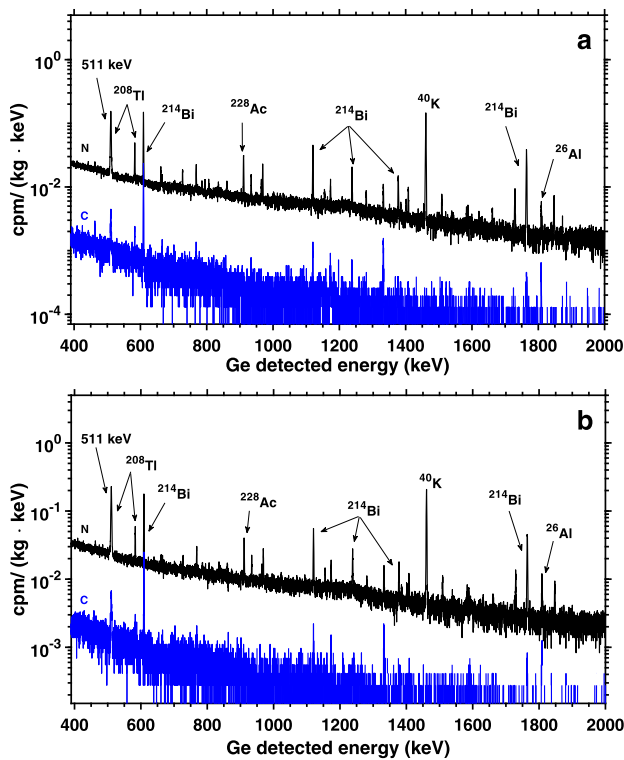


**Fig. 3** Ge spectra in normal mode (black) and in  $\beta^+$ —1022 keV coincidence mode (blue) for the two Gebel Kamil fragments (a) GK1 and (b) GK2. The cosmogenic  $^{26}\text{Al}$  peak and a few peaks from the background of naturally occurring potassium, uranium and thorium are marked

The detection efficiency of gamma rays of various energies emanating from a rock varies with the sample geometry, composition and density, *i.e.*, size, shape and constituent major elements. In case of chondrites, which have some inherent  $^{40}\text{K}$ , the full peak efficiency (FPE) can be calculated using its 1460.82 keV gamma ray emission rate and the FPE for other energy regions is scaled from the  $^{40}\text{K}$  efficiency, using their mass attenuation coefficients and detector characteristics. In case of iron meteorites no such internal radioactive nuclide is available for calibration. Therefore, the FPE values at different energy lines were experimentally determined by making two moulds for GK1 and GK2 having shapes identical to each of the fragments. The moulds were filled with labelled sediment having known amounts of  $^{60}\text{Co}$ ,  $^{40}\text{K}$ ,  $^{137}\text{Cs}$  and iron powder. Since the high density of Gebel Kamil ( $7.9\text{ g cm}^{-3}$ ) could not be achieved with iron powder, self-absorption effects were estimated on the basis of efficiency measurements of a set of moulds with different densities. The average attenuation length was estimated and used to calculate the efficiency correction for the actual density of the meteorite (Colombetti et al. 2013). The mass attenuation coefficient, as a function of energy, was obtained for a few elements that are relevant to meteorite compositions from the National Institute of Standards and

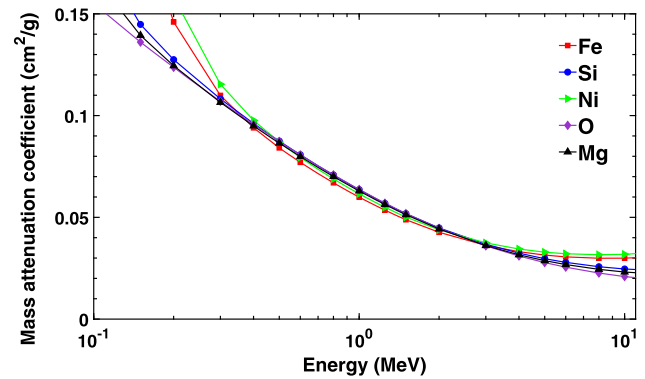


**Fig. 4** Mass attenuation coefficients for elements relevant to meteorite composition, obtained from NIST Standard Reference Database (Hubbell and Seltzer 1995)

Technology—Standard Reference Database 126 (Hubbell and Seltzer 1995). This technique (the use of moulds reproducing shape and density of the meteorite sample) relies on the fact that most of the measured gamma rays are in the energy range 300–3000 keV, where the mass attenuation coefficients for different atomic species differ, at most, by a few percent, as shown in Fig. 4.

### 3 Results and discussion

The gamma ray spectra of the two fragments GK1 and GK2 in normal and coincidence modes in the 400–2000 keV spectral range are shown in Fig. 3. The major peaks of the detected radionuclides are marked with arrows. The counting details of the two fragments and the background are given in Table 2.

#### 3.1 Activity due to $^{26}\text{Al}$

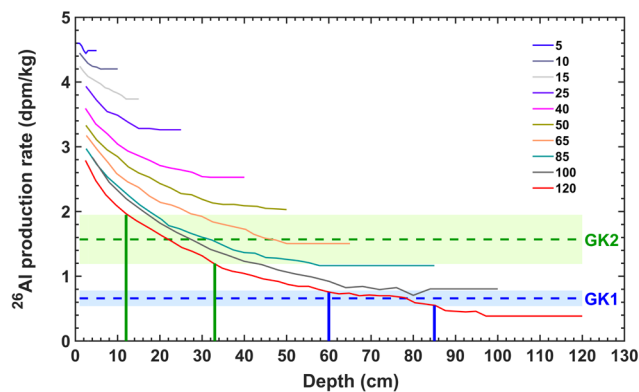
We find several gamma ray peaks in the spectra, as shown in Fig. 3, Most of them are due to the familiar U and Th decay products and  $^{40}\text{K}$ , which were also present in the background and hence were discarded. The only other significant peak (1808.65 keV) in the normal mode is due to  $^{26}\text{Al}$ , expected to be produced in cosmic ray interactions in the meteorite and resulting in a value of  $0.66 \pm 0.12$  dpm/kg meteorite for GK1 and  $1.57 \pm 0.38$  dpm/kg meteorite for GK2, respectively.

#### 3.2 Production rates and shielding parameters

The  $^{26}\text{Al}$  radionuclide is mainly produced by cosmic ray interactions with Fe and Ni nuclei contained in the meteorite. We use the *physical model* by Michel et al. (1991), based on High Energy Particle Transport code which was verified by measured depth profiles of several radionuclides

**Table 2** Counting data of samples GK1 and GK2 with associated  $1\sigma$  uncertainties

Sample	GK1		GK2	
Maximum dimensions	10 cm × 6 cm × 3 cm		8 cm × 6 cm × 4 cm	
Sample mass	672 g		450 g	
Counting time	80 days		55.8 days	
Isotope	$^{26}\text{Al}$	$^{44}\text{Ti}$	$^{26}\text{Al}$	$^{44}\text{Ti}$
Counting mode	normal	coincidence	normal	coincidence
	1809 keV (Ge)	1157 keV (Ge) + 1022 keV (NaI)	1809 keV (Ge)	1157 keV (Ge) + 1022 keV (NaI)
cpd <sup>a</sup> /kg	11.88 ± 0.72	<1	30.52 ± 1.45	< 2
Compton background <sup>b</sup>	1.75 ± 0.07	0.18 ± 0.02	1.53 ± 0.08	0.19 ± 0.03
dpm <sup>c</sup> /kg	0.66 ± 0.12	<0.05	1.57 ± 0.38	< 0.07

<sup>a</sup>cpd = count per day<sup>b</sup>cpd/keV<sup>c</sup>dpm = disintegrations per minute

**Fig. 5** Calculated  $^{26}\text{Al}$  production depth profiles for the Gebel Kamil composition in meteoroids with different pre-atmospheric radii (cm) given in the legend. The dashed blue and green lines and the corresponding error bands represent the  $^{26}\text{Al}$  activities measured in GK1 and GK2 respectively. The depth ranges deduced for GK1 (60–85 cm) and GK2 (12–33 cm) are also shown (blue and green vertical lines)

in stony meteorites having well determined preatmospheric sizes (Bhandari et al. 1993). Ammon et al. (2009) converted the same model by Michel et al. (1991) for iron meteorites and calculated the production profiles of several radionuclides and noble gases, which however do not match properly the experimental data over the entire range of depths. The production rates of nuclides depend on the size of the meteoroid and location within it and therefore the observed activity can be used to estimate the size of the meteoroid and shielding depth of different fragments. Figure 5 shows the  $^{26}\text{Al}$  depth profiles, calculated with the model of Michel et al. (1991), that we used to determine the preatmospheric size of Gebel Kamil of  $\sim 1$  meter and the shielding depths of GK1 and GK2 to cosmic rays within the meteoroid using the measured composition (Fe = 80.2%, Ni = 19.8%, P = 0.19% and S = 0.21%) as given by Folco et al. (2011)

and Gemelli et al. (2015). The  $^{26}\text{Al}$  activity measured here in GK1 and GK2 are 0.66 and 1.57 dpm/kg respectively. In view of the large cosmic ray exposure age (366 Ma),  $^{26}\text{Al}$  ( $T_{1/2} = 717$  ka) must have attained secular equilibrium in space and its decay over 3000 years of terrestrial age is negligible. We can therefore proceed with the measured values of  $^{26}\text{Al}$  and determine the shielding parameters. In Fig. 5, we show the  $^{26}\text{Al}$  values for GK1 (dashed-blue lines) and GK2 (dashed-green lines). The shaded region represents the  $1\sigma$  error band. The  $^{26}\text{Al}$  activity in GK2 is compatible with meteoroids with radius greater than 65 cm, while the lower activity in GK1 suggests radius of about 100 cm. Using this value, we deduce that the pre-atmospheric mass of Gebel Kamil meteorite should have been greater than 30 tons and could be about 60 tons. This estimate can be compared with estimates of 20–40 tons based on the work of Folco et al. (2010), Bland and Artemieva (2006) and Ott et al. (2014).

Several cosmogenic radioisotopes ( $^{10}\text{Be}$ ,  $^{26}\text{Al}$ ,  $^{36}\text{Cl}$ ,  $^{41}\text{Ca}$ ,  $^{53}\text{Mn}$ , and  $^{60}\text{Fe}$ ) in some other fragments of Gebel Kamil meteorite have been measured earlier by Ott et al. (2014). They find that the measured activity of some radioisotopes in smaller fragments and shrapnels is a factor of  $\sim 3$  (for the longer lived radionuclide  $^{53}\text{Mn}$ ) or  $\sim 5$  (for shorter lived  $^{41}\text{Ca}$  and  $^{60}\text{Fe}$ ) lower compared to that in the main mass, indicating that the main mass was located at shallower depth and shrapnels originated from deep inside the meteoroid.  $^{26}\text{Al}$  in the four samples measured also varies by more than a factor 4, between 0.215 in shrapnels and 1.049 dpm/kg in the main mass. Thus our data broadly confirm that the main mass was less shielded compared to shrapnels. The  $^{26}\text{Al}$  of 1.57 dpm/kg measured here in GK2 is the highest value found so far in this meteorite and is about 2.3 times higher than 0.66 dpm/kg measured in GK1 and over 7 times higher than the minimum value of 0.215 dpm/kg found in a fragment (Ott et al. 2014). These variations in

shrapnels and the main mass are consistent with the rare gas and radionuclide data of Ott et al. (2014). The higher values in GK2 indicate that the sample experienced small shielding and was closer to the surface irradiated by cosmic rays in space. The average depth is estimated to be about 73 cm ( $\sim 580 \text{ g cm}^{-2}$ ) for GK1 and 22 cm ( $\sim 170 \text{ g cm}^{-2}$ ) for GK2 and, under assumption of spherical shape, the meteoroid had a radius of 1.2 meters in space (Ott et al. 2014).

### 3.3 Complications arising from asymmetric ablation

The absence or presence of ablation features such as fusion crust and regmaglypts enables us to reconstruct the complicated history of a meteorite's transit through the atmosphere. As can be seen from Fig. 1, GK1 has a relatively smooth surface with flattish and roughly irregular-rectangular faces with no regmaglypts on its surface, indicating that it is an interior piece and was broken, not in the atmosphere but due to impact on the ground. In comparison, the smaller fragment GK2 was cut from the narrowest edge of the largest fragment (Fig. 2), the main mass, weighing 83 kg. It has elongated mace-like shape, with one end (S) (from where the sample was taken) considerably thinned out and the opposite end (L) has a wider, hemispherical shape. This main mass is covered all over with regmaglypts, with roundish face (L) opposite to GK2, having well developed, large regmaglypts and dark and shiny complexion, as a consequence of severe heating and ablation. Based on the arguments developed from study of shapes of meteorites (Bhandari et al. 1980), we can conclude that (i) the mace like shape of the *individual* shows that the surface S had the smallest pre-atmospheric depth, while the larger basal face L had the largest one (Bhandari et al. 1980); (ii) this fragment had an oriented entry, with S as the rear end and L as the leading end during its transit through the Earth's atmosphere.

There has been much debate whether the meteoroid broke up in the atmosphere or on impact on the ground. All the small fragments (shrapnels) were found in a narrow cluster and very few of them have ablation features (thumb prints and fusion crust), indicating that their parent body broke only upon impact on the ground. In addition, due to the absence of companion craters and since fragments were found in a close cluster, Folco et al. (2010, 2011) concluded that the Gebel Kamil meteorite impacted the ground either as a single mass or as a tight cluster of fragments, with only minor fragmentation and separation during atmospheric flight. It can be visualized that before fragmentation, the meteoroid must have survived multiple fractures in space or on the parent body, which made it easy for it to break up into such a large number of fragments. On the other hand, mace (or bell) like shape of the 83 kg main mass (the *individual*) and well-developed ablation features all over its surface (Fig. 2) suggest that at least this fragment separated from the meteorite body in the atmosphere, before impact. Breaking up

of the meteoroid in two bodies, *i.e.* the parent body of the shrapnels and the main mass, must have occurred at low altitude because they were found close by, only 200 meters apart from each other. Our study indicates that the larger body broke into thousands of pieces upon impact, whereas the other body, which resulted in the main mass, separated in the atmosphere before the impact.

The shielding overburden calculated in Sect. 3.2 is for symmetric ablation (case I or II of Bhandari et al. 1980). If the ablation is asymmetric (case III or IV), the estimates of shielding depth would be erroneous. We must therefore consider 'average' shielding depth which depends on the average ablation and 'effective' shielding depths, which also take into account the profiles of the cosmic ray products with which we are concerned here. We have calculated average shielding depth of 22 cm for GK2, based on its  $^{26}\text{Al}$  activity. Considering that the size of the fragment is  $10 \times 6 \times 3 \text{ cm}$ , it is possible that the effective shielding was less than 12 cm.

### 3.4 $^{44}\text{Ti}$ and terrestrial age

For the purpose of determining  $^{44}\text{Ti}$  production profiles in these iron meteorites, we have followed the model of Neumann et al. (1997), as previously done for stony meteorites (Taricco et al. 2006). We expect its activity at the time of fall between 1.6 and 2.6 dpm/kg in the two fragments respectively, using the above shielding parameters. However, we did not find any measurable activity. Presumably all the  $^{44}\text{Ti}$  produced during cosmic ray exposure has decayed during its residence on the Earth and therefore the terrestrial age must be greater than a few centuries. Absence of  $^{44}\text{Ti}$  activity thus provides a lower limit for the terrestrial age of  $>300$  years. Based on archaeological evidence, as well as geological evidence (lack of erosion, well preserved crater rim etc.), it was concluded that the crater probably formed less than 5000 years ago (Folco et al. 2011). Based on thermoluminescence dating, Sighinolfi et al. (2015) gave a better and more reliable estimate and concluded that the date of the impact was between 1600 and 400 BC ( $2\sigma$ ). The absence of  $^{44}\text{Ti}$  activity is consistent with this estimate.

## 4 Conclusions

We have measured the gamma activity of two large fragments of the Gebel Kamil meteorite using a double detector gamma-ray coincidence spectrometer. The activity of  $^{26}\text{Al}$  in GK2 is 1.57 dpm/kg meteorite compared to GK1 which has 0.66 dpm/kg meteorite, indicating that GK2, which was part of the main mass, was exposed to higher cosmic ray flux and must have been located closer to the surface of the meteoroid, whereas the shrapnel (GK1) was located deep within the meteoroid. In particular, the average shielding depth of

samples within the meteoroid during its cosmic ray exposure was  $\sim 73$  cm (for GK1) and  $\sim 22$  cm (for GK2) respectively but the effective depth of the nearest face of the samples from the exposed surface of the meteoroid could be as low as 68 cm (GK1) and  $< 12$  cm (for GK2) respectively. These data suggest that the pre-atmospheric mass of the meteorite was 30 to 60 tons and the main mass had an oriented entry, having suffered little ablation at the location from where GK2 was broken off. The ablation of the meteorite was highly asymmetric. Our study suggests that the meteoroid fragmented in the atmosphere; the bigger fragment broke into a large number of shrapnels on impact on the ground and the other fragment (main mass), having ablation features all around, remained intact. All the  $^{44}\text{Ti}$  activity seems to have decayed since the fall, indicating a terrestrial age of  $> 3$  centuries.

**Acknowledgements** We are grateful to Dr. R. Michel for giving us the procedures for calculating production rates of nuclides in meteorites. We thank Dr. U. Ott for his precious suggestions which enabled us to improve the paper.

**Funding Information** The authors state that they have not received any research grants.

**Conflict of interest** The authors declare that they have no conflict of interest.

**Publisher's Note** Springer Nature remains neutral with regard to jurisdictional claims in published maps and institutional affiliations.

## References

- Ammon, K., Masarik, J., Leya, I.: *Meteorit. Planet. Sci.* **44**, 485 (2009). <https://doi.org/10.1111/j.1945-5100.2009.tb00746.x>
- Asvestari, E., Usoskin, I.G., Kovaltsov, G.A., Owens, M.J., Krivova, N.A., Rubinetti, S., Taricco, C.: *Mon. Not. R. Astron. Soc.* **467**, 1608 (2017). <https://doi.org/10.1093/mnras/stx190>
- Bhandari, N., Lal, D., Rajan, R.S., Arnold, J.R., Marti, K., Moore, C.B.: *Nucl. Tracks* **4**, 213 (1980)
- Bhandari, N., Mathew, K.J., Rao, M.N., Herpers, U., Bremer, K., Vogt, S., Wölfli, W., Hofmann, H.J., Michel, R., Bodemann, R., Lange, H.-J.: *Geochim. Cosmochim. Acta* **57**, 2361 (1993). [https://doi.org/10.1016/0016-7037\(93\)90574-G](https://doi.org/10.1016/0016-7037(93)90574-G)
- Bland, P.A., Artemieva, N.A.: *Meteorit. Planet. Sci.* **41**, 607 (2006). <https://doi.org/10.1111/j.1945-5100.2006.tb00485.x>
- Colombetti, P., Taricco, C., Bhandari, N., Romero, A., Verma, N., Vivaldo, G.: In: *IEEE Nuclear Science Symposium Conference Record, 2008 (NSS'08)*, p. 1802 (2008)
- Colombetti, P., Taricco, C., Bhandari, N., Sinha, N., Di Martino, M., Cora, A., Vivaldo, G.: *Nucl. Instrum. Methods Phys. Res., Sect. A, Accel. Spectrom. Detect. Assoc. Equip.* **718**, 140 (2013). <https://doi.org/10.1016/j.nima.2012.07.053>
- Di Martino, M., Taricco, C., Colombetti, P., Cora, A., Mancuso, S.: *Mem. Soc. Astron. Ital. Suppl.* **26**, 62 (2014)
- D'Orazio, M., Folco, L., Zeoli, A., Cordier, C.: *Meteorit. Planet. Sci.* **46**, 1179 (2011). <https://doi.org/10.1111/j.1945-5100.2011.01222.x>
- Folco, L., Di Martino, M., El Barkooby, A., D'Orazio, M., Lethy, A., Urbini, S., Nicolosi, I., Hafez, M., Cordier, C., van Ginneken, M., Zeoli, A., Radwan, A.M., El Khrepy, S., El Gabry, M., Gomaa, M., Barakat, A.A., Serra, R., El Sharkawi, M.: *Science* **329**, 804 (2010). <https://doi.org/10.1126/science.1190990>
- Folco, L., Di Martino, M., El Barkooby, A., D'Orazio, M., Lethy, A., Urbini, S., Nicolosi, I., Hafez, M., Cordier, C., van Ginneken, M., Zeoli, A., Radwan, A.M., El Khrepy, S., El Gabry, M., Gomaa, M., Barakat, A.A., Serra, R., El Sharkawi, M.: *Geology* **39**, 179 (2011). <https://doi.org/10.1130/G31624.1>
- Folco, L., D'Orazio, M., Fazio, A., Cordier, C., Zeoli, A., Ginneken, M., El-Barkooby, A.: *Meteorit. Planet. Sci.* **50**, 382 (2015). <https://doi.org/10.1111/maps.12427>
- Gemelli, M., D'Orazio, M., Folco, L.: *Geostand. Geoanal. Res.* **39**(1), 55 (2015)
- Hubbell, J.H., Seltzer, S.M.: *Tables of X-ray mass attenuation coefficients and mass energy-absorption coefficients 1 keV to 20 MeV for elements Z = 1 to 92 and 48 additional substances of dosimetric interest. Technical report, National Inst. of Standards and Technology-PL, Gaithersburg, MD (United States). Ionizing Radiation Div. (1995)*
- Mancuso, S., Taricco, C., Colombetti, P., Rubinetti, S., Sinha, N., Bhandari, N.: *Astron. Astrophys.* **610**, 28 (2018). <https://doi.org/10.1051/0004-6361/201730392>. [arXiv:1801.01311](https://arxiv.org/abs/1801.01311)
- Michel, R., Dragovitsch, P., Cloth, P., Dagge, G., Filges, D.: *Meteoritics* **26**, 221 (1991)
- Neumann, S., Leya, I., Michel, R.: *Meteorit. Planet. Sci.* **32**, A98 (1997)
- Ott, U., Merchel, S., Herrmann, S., Pavetich, S., Rugel, G., Faestermann, T., Fimiani, L., Gomez-Guzman, J.M., Hain, K., Korschinek, G., Ludwig, P., D'Orazio, M., Folco, L.: *Meteorit. Planet. Sci.* **49**, 1365 (2014). <https://doi.org/10.1111/maps.12334>
- Sighinolfi, G.P., Sibilina, E., Contini, G., Martini, M.: *Meteorit. Planet. Sci.* **50**, 204 (2015). <https://doi.org/10.1111/maps.12417>
- Taricco, C., Bhandari, N., Cane, D., Colombetti, P., Verma, N.: *J. Geophys. Res. Space Phys.* **111**, 08102 (2006). <https://doi.org/10.1029/2005JA011459>
- Taricco, C., Bhandari, N., Colombetti, P., Verma, N., Vivaldo, G.: *Nucl. Instrum. Methods Phys. Res., Sect. A, Accel. Spectrom. Detect. Assoc. Equip.* **572**, 241 (2007). <https://doi.org/10.1016/j.nima.2006.10.359>
- Taricco, C., Bhandari, N., Colombetti, P., Verma, N.: *Adv. Space Res.* **41**, 275 (2008). <https://doi.org/10.1016/j.asr.2007.06.050>
- Taricco, C., Sinha, N., Bhandari, N., Colombetti, P., Mancuso, S., Rubinetti, S., Barghini, D.: *Astrophys. Space Sci.* **361**, 338 (2016). <https://doi.org/10.1007/s10509-016-2909-7>
- Usoskin, I.G., Solanki, S.K., Taricco, C., Bhandari, N., Kovaltsov, G.A.: *Astron. Astrophys.* **457**, 25 (2006). <https://doi.org/10.1051/0004-6361:20065803>